International Symposium on Information Theory and its Applications, ISITA2008
Auckland, New Zealand, 7-10, December, 2008

# On Logarithmic Spherical Vector Quantization

Hauke Krüger, Raimund Schreiber, Bernd Geiser, and Peter Vary

Institute of Communication Systems and Data Processing (IND), RWTH Aachen University
52056 Aachen, Germany
E-mail: {krueger,schreiber,geiser,vary}@ind.rwth-aachen.de

**Abstract**

Logarithmic spherical vector quantization (LSVQ) is a specific type of gain-shape vector quantization (VQ), where input vectors are decomposed into a gain and a shape component which are quantized independently. In this contribution, novel theoretical results on LSVQ are presented: It will be shown that, for high bit rates, with logarithmic (A-Law) scalar quantization (SQ) of the gain and spherical vector quantization (SVQ) of the shape component a signal-to-noise ratio (SNR) is achieved which is approximately independent of the input source distribution. In addition, a detailed theoretical analysis leads to a lower bound for the quantization distortion related to SVQ. By introducing approximations for the assumption of high bit rates, this bound is the basis for the computation of the optimal allocation of bit rate to the gain and the shape quantizer, respectively, and yields an estimate for the achievable SNR for LSVQ.

## 1. Introduction

In quantization [1], apart from the achievable performance, also computational complexity and memory consumption are traditionally of high importance for practical applications. On the one hand, fixed-rate SQ [2] is known to require low computational complexity and memory. On the other hand, it was shown that SQ is outperformed by fixed-rate VQ which benefits from the *space filling*, the *shape* and the *memory advantage* [3]. Techniques such as gain-shape [4], lattice based [5] and permutation code [6] VQ have been proposed, offering a reasonable balance between quantization performance and coding complexity. In many cases, VQs are designed under the assumption of a specific simple source distribution and, in particular, for memoryless sources. If the distribution of the input source is unknown, the assumption of a Gaussian distribution is useful as a worst case scenario since it has the highest differential entropy [7]. Targeting high coding efficiency, gain-shape VQ based on spherical vector quantization (SVQ) of the shape part, with all codevectors located on the surface of scaled versions of the unit sphere, well approximates the optimal codevector density for a Gaussian source. Applications of gain-shape SVQ for source coding have been proposed in numerous publications, e.g., [8] and [9]. Remarkable results on the analysis of spherical codes in general are in particular given in [10]. In [11], SVQ based on a so-called wrapped spherical code is combined with source optimized SQ in gain-shape fashion for the coding of Gaussian sources.
In this paper, we present a theoretical analysis of LSVQ which, in contrast to the work in [11], is based on a combination of SVQ with logarithmic SQ. The employment of a logarithmic rather than a source optimized SQ is motivated by the fact that the variance of input signals in practice reveals a wide dynamic range. As a novel result, it will be shown in Section 2 that LSVQ approximately achieves a constant quantization SNR independent of the probability density function (PDF) of the input source over a wide dynamic range for high bit rates. In Section 3, very similar to the sphere bound for VQ in general [12], a lower bound for the achievable quantization distortion related to SVQ and a high rate estimate for the theoretical performance of LSVQ are derived. Integral part of the derivation of the high rate estimate is the calculation of the optimal allocation of bit rate to the gain and shape components. SNR curves for LSVQ will be presented in Section 4.

## 2. Logarithmic Spherical Vector Quantization

A vector quantizer (VQ) is an entity that maps an $L_v$-dimensional input vector $\mathbf{x} \in \mathbb{R}^{L_v}$ to a vector representative taken from a finite vector codebook $\mathcal{X}$ to produce the quantized vector $\tilde{\mathbf{x}} = Q_{\mathrm{vq}}(\mathbf{x}) \in \mathcal{X}$. In the quantization process, the goal is to select that codevector $\tilde{\mathbf{x}}$ which minimizes a specific quantization distortion, in the following the squared error

$$d(\mathbf{x}, \tilde{\mathbf{x}}) = \| \mathbf{x} - \tilde{\mathbf{x}} \|_2^2 \, . \tag{1}$$

LSVQ is a special type of VQ in which each input vector is decomposed into its absolute value and a normalized

version with unit absolute value, referred to as the gain and the shape components

$$g = \| \mathbf{x} \|_2 \qquad \text{and} \qquad \mathbf{c} = \frac{1}{g} \cdot \mathbf{x}. \tag{2}$$

Both components are quantized independently by logarithmic SQ according to the A-Law rule [2] and SVQ to produce the quantized versions $\tilde{g} = Q_g(g)$ and $\tilde{\mathbf{c}} = Q_{\text{svq}}(\mathbf{c})$, respectively. The input signal is reconstructed to produce the overall quantized signal vector

$$\tilde{\mathbf{x}} = \tilde{\mathbf{c}} \cdot \tilde{g}. \tag{3}$$

The independent quantization of gain and shape component enables a very efficient realization. Given the *effective bit rate* (the number of bits per vector coordinate) for the two quantizers as $r_g$ and $r_{\text{svq}}$, the number of quantization reconstruction levels of $Q_g$ is $N_g = 2^{r_g \cdot L_v}$, and the number of *spherical codevectors* related to $Q_{\text{svq}}$ is $N_{\text{svq}} = 2^{r_{\text{svq}} \cdot L_v}$, respectively. The overall number of codevectors related to the combination of both quantizers, referred to as *overall codevectors*, is

$$N_{\text{lsvq}} = 2^{r_{\text{lsvq}} \cdot L_v} = N_g \cdot N_{\text{svq}} = 2^{(r_{\text{svq}} + r_g) \cdot L_v} \tag{4}$$

with the overall effective bit rate $r_{\text{lsvq}}$. All normalized vectors $\mathbf{c}$ to be quantized by $Q_{\text{svq}}$ are located on the surface of an $L_v$-dimensional sphere with radius $R = 1.0$, denoted as $\mathcal{S}_{L_v}^{(1.0)}$. Given the spherical vector codebook $\mathcal{C}_{\text{svq}}$ for $Q_{\text{svq}}$, the *spherical quantization cells* are defined as

$$C_{\tilde{\mathbf{c}}} = \{\mathbf{c} \in \mathcal{S}_{L_v}^{(1.0)} : \| \mathbf{c} - \tilde{\mathbf{c}} \|_2^2 \leq \| \mathbf{c} - \tilde{\mathbf{c}}' \|_2^2 \quad \forall\, \tilde{\mathbf{c}}' \neq \tilde{\mathbf{c}}, \text{ and } \tilde{\mathbf{c}}', \tilde{\mathbf{c}} \in \mathcal{C}_{\text{svq}}\}. \tag{5}$$

For the first part of the analysis of LSVQ, all spherical quantization cells are assumed to be of identical shape. The overall surface area content of a sphere in $L_v$ dimensions with radius $R$ is

$$S_{\mathcal{S}_{L_v}} = V_{\mathcal{S}_{L_v}}^{(1.0)} \cdot L_v \cdot R^{(L_v - 1)} \tag{6}$$

with $V_{\mathcal{S}_{L_v}}^{(1.0)}$ as the volume of an $L_v$-dimensional unit sphere [13],

$$V_{\mathcal{S}_{L_v}}^{(1.0)} = \frac{2 \cdot \pi^{L_v/2}}{L_v \cdot \Gamma(\frac{L_v}{2})}, \tag{7}$$

and the $\Gamma$-function defined, e.g., in [14]. The content of each single spherical quantization cell on the surface of the *unit* sphere can be computed as

$$S_{C_{\tilde{\mathbf{c}}}}^{(I)} = \frac{S_{\mathcal{S}_{L_v}}}{N_{\text{svq}}} = \frac{2 \cdot \pi^{L_v/2}}{\Gamma(\frac{L_v}{2}) \cdot N_{\text{svq}}}. \tag{8}$$

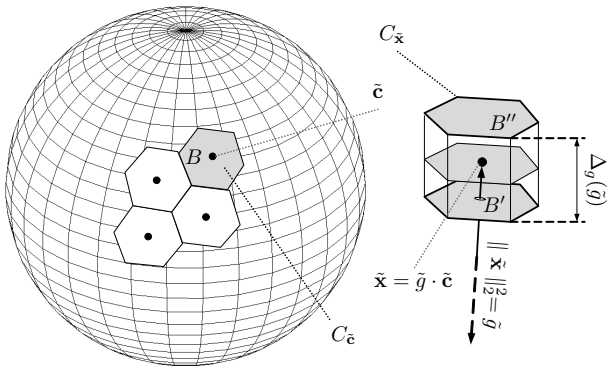


Figure 1: Spherical quantization cells located on the surface of the unit sphere (left side) and example overall quantization cell (right side) for $L_v = 3$.

The covering of the sphere surface for $L_v = 3$ is demonstrated on the left side of Figure 1. For the construction of the overall codevectors $\tilde{\mathbf{x}}$ according to (3), the spherical codevectors are combined with different quantization reconstruction levels $\tilde{g}$, and *overall quantization cells* $C_{\tilde{\mathbf{x}}}$ result. On the right side of Figure 1, an example overall quantization cell is shown for $L_v = 3$. Compared to the "flat" spherical quantization cells ($B$ in the figure), the overall quantization cells also have a height in radial direction which is the distance between adjacent radius quantization reconstruction levels, denoted as $\Delta_g(\tilde{g})$. The bottom and the upper side surface areas of that cell, $B'$ and $B''$, respectively, are scaled versions of the spherical quantization cells, $B$. For high bit rates and hence a large number of codevectors, the curvature of the sphere can be neglected, and $\Delta_g(\tilde{g})$ is small. In this case, the bottom and the upper side surface area of the overall quantization cell are approximately identical (therefore $B' \approx B''$ in Figure 1). With the overall codevector $\tilde{\mathbf{x}}$ located in the center of the quantization cell, the sphere radius scaling factor is $\tilde{g} = \| \tilde{\mathbf{x}} \|_2$ so that $B' \approx B'' \approx B \cdot \tilde{g}^{(L_v - 1)}$ (6), and the cell volume is approximately

$$V_{C_{\tilde{\mathbf{x}}}}(\tilde{g}) \approx S_{C_{\tilde{\mathbf{c}}}}^{(I)} \cdot \tilde{g}^{(L_v - 1)} \cdot \Delta_g(\tilde{g}). \tag{9}$$

Assuming that the gain factors to be quantized fall into the logarithmic area of the A-Law compression curve, $\Delta_g(\tilde{g})$ is approximately the quantization error related to A-Law quantization of the radius [2],

$$\Delta_g(\tilde{g}) = \frac{(1 + \ln(A))}{N_g} \cdot \tilde{g} \tag{10}$$

with $A$ as the A-Law quantization constant. Hence, the overall quantization cell volume is approximately

$$V_{C_{\tilde{\mathbf{x}}}}(\| \tilde{\mathbf{x}} \|_2) \approx \frac{2 \cdot \pi^{L_v/2} \cdot (1 + \ln(A))}{\Gamma(L_v/2)} \cdot \frac{(\| \tilde{\mathbf{x}} \|_2)^{L_v}}{N_{\text{svq}} \cdot N_g} \tag{11}$$

and is a function of the absolute value of the corresponding overall codevector, $\| \tilde{\mathbf{x}} \|_2 = \tilde{g}$. From this cell volume, the quantizer point density function can be derived as

$$\lambda(\tilde{\mathbf{x}}) \approx \frac{\Gamma(L_v/2)}{2 \cdot \pi^{L_v/2} \cdot (1 + \ln(A))} \cdot (\| \tilde{\mathbf{x}} \|_2)^{-L_v}. \quad (12)$$

Given $p(\mathbf{x})$ as the PDF of the input signal source, it is a common assumption in high bit rate VQ that $p(\mathbf{x}) \approx p(\tilde{\mathbf{x}})$ and $\lambda(\tilde{\mathbf{x}})$ is a continuous function. According to [12], it follows that the mean of the overall quantization distortion can be computed from (12) as

$$D_{\text{lsvq}}^{(I)} = N_{\text{lsvq}}^{-2/L_v} \cdot C_{\text{lsvq}} \cdot \int_{\tilde{\mathbf{x}} \in \mathbb{R}^{L_v}} \frac{p(\tilde{\mathbf{x}})}{(\lambda(\tilde{\mathbf{x}}))^{2/L_v}} \mathrm{d}\tilde{\mathbf{x}}. \quad (13)$$

Correspondingly, the SNR is

$$\begin{aligned} \text{SNR}_{\text{lsvq}}^{(I)} = & \frac{N_{\text{lsvq}}^{2/L_v}}{C_{\text{lsvq}} \cdot \pi} \cdot \left( \frac{\Gamma(L_v/2)}{2 \cdot (1 + \ln(A))} \right)^{2/L_v} \\ & \cdot \underbrace{\frac{\int_{\mathbf{x} \in \mathbb{R}^{L_v}} p(\mathbf{x}) \cdot \| \mathbf{x} \|_2^2 \cdot \mathrm{d}\mathbf{x}}{\int_{\tilde{\mathbf{x}} \in \mathbb{R}^{L_v}} p(\tilde{\mathbf{x}}) \cdot \| \tilde{\mathbf{x}} \|_2^2 \cdot \mathrm{d}\tilde{\mathbf{x}}}}_{\approx 1} \end{aligned} \quad (14)$$

with constant $C_{\text{lsvq}}$ in (13) and (14) depending on the (yet unknown) shape of the overall quantization cells. As conclusion, the SNR related to LSVQ is approximately independent of the PDF of the input signal.

## 3. Analysis of an "Idealized" SVQ

With respect to the assumptions and the proof of a constant SNR in the previous section, w.l.o.g. only a single overall quantization cell is regarded in the following with the corresponding overall codevector located on the surface of the unit sphere ($\| \tilde{\mathbf{x}} \|_2 = 1$). A quantitative expression for the SNR rather than the qualitative one as in (14) shall be derived. For this purpose, the quantization distortion solely related to $Q_{\text{svq}}$ will be computed at first and then combined with the distortion related to $Q_g$.

Since the exact shape of the spherical quantization cells is unknown, in analogy to the sphere bound for VQ in general [12], we define an "idealized" SVQ to be composed of "spherical cap" quantization cells as illustrated by Figure 2 for $L_v = 3$. The spherical codevector $\tilde{\mathbf{c}}$ is located in the center (at the north pole), and the angular radius $\gamma$ determines the size of the spherical cap. The spherical cap area content [10] is

$$S_{C_{\tilde{\mathbf{c}}}}^{(II)} = V_{\mathcal{S}_{L_v-1}}^{(1.0)} \cdot (L_v - 1) \cdot \int_0^{\gamma} (\sin(\beta))^{(L_v-2)} \mathrm{d}\beta. \quad (15)$$

Note that the extension $(II)$ is used here to highlight the difference to the cell area content in (8).

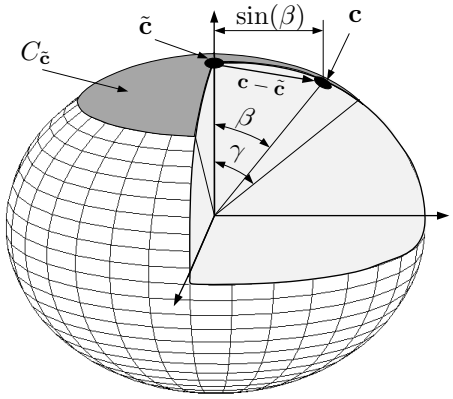


Figure 2: "Spherical cap" quantization cell, $L_v = 3$.

Given a normalized vector $\mathbf{c}$ which is located inside the spherical cap area as shown in the example of Figure 2, the absolute value of the quantization error can be computed as a function of $\beta$,

$$\| \mathbf{c} - \tilde{\mathbf{c}} \|_2 = 2 \cdot \sin(\beta/2). \quad (16)$$

Assuming that the distribution of $\mathbf{c}$ within the spherical cap quantization cell is uniform (constant PDF $p(\mathbf{c})$), the distortion as a function of angular radius $\gamma$ is

$$\begin{aligned} D_{\text{svq}} &= \int_{C_{\tilde{\mathbf{c}}}} p(\mathbf{c}) \cdot \| \mathbf{c} - \tilde{\mathbf{c}} \|_2^2 \, \mathrm{d}\mathbf{c} \\ &= \frac{\int_0^{\gamma} (2 \cdot \sin(\frac{\beta}{2}))^2 \cdot (\sin(\beta))^{(L_v-2)} \mathrm{d}\beta}{\int_0^{\gamma} (\sin(\beta))^{(L_v-2)} \mathrm{d}\beta} \end{aligned} \quad (17)$$

with

$$p(\mathbf{c}) = 1 / S_{C_{\tilde{\mathbf{c}}}}^{(II)}. \quad (18)$$

So far, $\gamma$ is the unknown parameter in (17). In order to compute this parameter, it is assumed that the complete unit sphere surface is covered by spherical cap quantization cells as shown on the left side of Figure 3. Given the angular radius such that the spherical caps do not overlap, the spheres do only cover a fraction of the complete surface. This approach is the analogon to "sphere packing" in the literature and demonstrated by Figure 3 a). The density $\delta \leq 1$ [5] depends on the vector dimension and is approximately the ratio between the area covered by spherical caps and the unit sphere surface area [10].

If no uncovered space is allowed, the spherical caps overlap as shown in Figure 3 b) which is the analogon to "sphere covering" in the literature. In analogy to the definition of the density, the thickness $\theta \geq 1$ is defined as the proportion of the overall space covered by the spherical caps in relation to the surface area of the unit sphere.

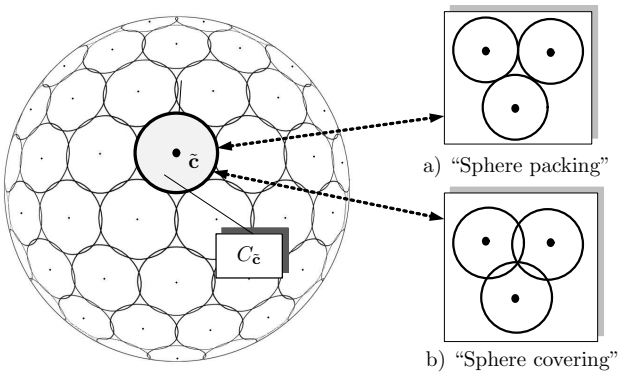


Figure 3: Covering of unit sphere surface by "spherical cap" quantization cells.

It is known that spheres have the lowest "moment of inertia" which is the basis for the derivation of the "sphere lower bound" for VQ in general [12]. Since the spherical quantization cells are restricted to be located on the surface of the unit sphere here, in analogy to the sphere as the optimum cell shape in VQ (due to the lowest "moment of inertia"), the spherical cap is the optimal cell shape in SVQ.
If the angular radius $\gamma$ is determined according to the "sphere packing" assumption, the distortion (17) is certainly lower than the distortion achievable by any distribution of codevectors on the sphere surface, referred to as "realistic" SVQ: The spherical quantization cells of the "idealized" SVQ have the optimal shape and also are smaller than those achievable in a "realistic" SVQ. In contrast to this, in the "sphere covering" approach, even though the cell shape is optimal, the distortion (17) is not a bound because the cells are larger than for a "realistic" SVQ.
The best option to compute $\gamma$, however, is to define that the spherical caps do not overlap and cover the complete surface at the same time. This assumption is obviously unrealistic as shown for the example $L_v = 3$ in Figure 3 but is the basis for a more accurate bound than that related to the "sphere packing" assumption: Since the area content related to the best "realistic" SVQ may be equal to that related to the "idealized" SVQ, the "idealized" SVQ has no benefit due to smaller spherical quantization cells. Nevertheless, the distortion is lower since the "idealized" SVQ benefits from the optimal spherical quantization cell shape which can not be achieved by a "realistic" SVQ for finite dimensions. This makes equation (17) to a lower bound which is more meaningful than the lower bound for the "sphere packing" approach.
Taking this into account, $\gamma$ can be computed from

$$S_{\mathcal{S}_{L_v}} = N_{\text{svq}} \cdot S_{\mathcal{C}_{\tilde{\mathbf{c}}}^{(II)}}. \tag{19}$$

Substituting (15) in (19) yields an equation from which the angular radius $\gamma$ can be determined. Due to the integral, a direct computation is not straight forward. It can, however, be solved numerically, e.g., by means of *Newtons Method*. Given the computed angular radius $\gamma$, the quantization distortion can be calculated by numerically solving the integrals (17).

### 3.1. High Bit Rate Approximations

For high bit rates, the angular radius $\gamma$ is very small, and the curvature of the sphere can be neglected. Considering the integral equations (15) and (17), the following approximations can be introduced,

$$\sin(\beta) \lesssim \beta \quad \text{for} \quad 0 \leq \beta \leq \gamma \tag{20}$$
$$2 \cdot \sin(\beta/2) \lesssim \beta \quad \text{for} \quad 0 \leq \beta \leq \gamma. \tag{21}$$

Correspondingly, the approximated angular radius is

$$\hat{\gamma} = \left( \frac{2\sqrt{\pi} \cdot \Gamma(\frac{L_v+1}{2})}{\Gamma(\frac{L_v}{2}) \cdot N_{\text{svq}}} \right)^{\frac{1}{L_v-1}}, \tag{22}$$

and the high rate approximation of the distortion (17) can be computed as

$$\hat{D}_{\text{svq}} = \frac{L_v - 1}{L_v + 1} \cdot \hat{\gamma}^2 = \frac{C_{\text{svq}}}{N_{\text{svq}}^{\frac{2}{L_v-1}}} \tag{23}$$

with the constant

$$C_{\text{svq}} = \frac{L_v - 1}{L_v + 1} \cdot \left( \frac{2\sqrt{\pi} \cdot \Gamma(\frac{L_v+1}{2})}{\Gamma(\frac{L_v}{2})} \right)^{\frac{2}{L_v-1}}. \tag{24}$$

The quantization of the gain factor can be considered as an error vector in radial direction which leads to the distortion [2]

$$D_g = \frac{C_g}{N_g^2} \quad \text{with} \quad C_g = \frac{(1 + \ln(A))^2}{12}. \tag{25}$$

As the curvature of the sphere is negligible for high bit rates, within each overall quantization cell, the error vector related to $Q_{\text{svq}}$, $\mathbf{c} - \tilde{\mathbf{c}}$, and that related to $Q_g$ are orthogonal and therefore independent. This allows that the corresponding quantization distortions can be added to yield the overall distortion

$$D_{\text{lsvq}}^{(II)} = \frac{C_{\text{svq}}}{N_{\text{svq}}^{\frac{2}{L_v-1}}} + \frac{C_g}{N_g^2}. \tag{26}$$

By using the approximations rather than the exact solution, with respect to (17), it can not be guaranteed that (26) is a bound. Therefore, all high rate results must be considered as a performance estimate for LSVQ rather than a bound.

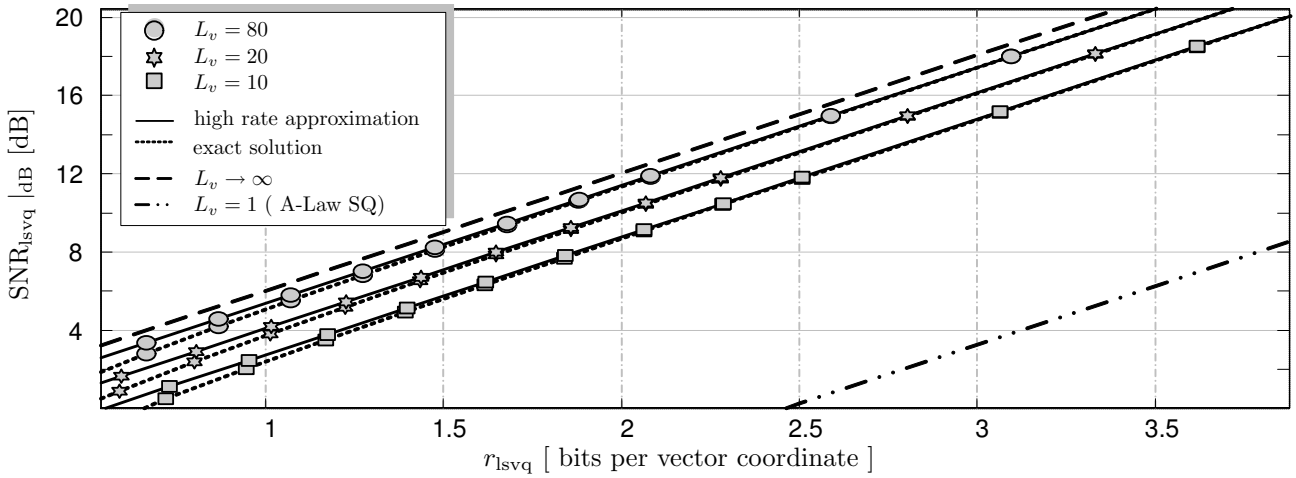


Figure 4: LSVQ quantization SNR in dB for different effective bit rates and dimensions. References for $L_v = 1$ and the asymptotic SNR for $L_v \to \infty$ (6-dB-per-bit rule) are shown. The A-Law constant is $A = 5000$.

### 3.2. Optimal Bit Allocation

In order to find the optimal distribution of the overall bit rate to $Q_g$ and $Q_{\mathrm{svq}}$, the overall distortion (26) is minimized in a Lagrangian optimization, given the constraint $N_{\mathrm{lsvq}} = N_{\mathrm{svq}} \cdot N_g$ in (4). The auxiliary function is

$$\chi = \frac{C_{\mathrm{svq}}}{N_{\mathrm{svq}}^{\frac{2}{L_v-1}}} + \frac{C_g}{N_g^2} + \lambda \cdot (N_g \cdot N_{\mathrm{svq}} - N_{\mathrm{lsvq}}). \quad (27)$$

Setting its partial derivatives with respect to $N_g$ and $N_{\mathrm{svq}}$ to zero yields

$$D_g = \frac{D_{\mathrm{svq}}}{L_v - 1} \quad (28)$$

as an intermediate result. The optimal number of spherical codevectors and gain quantization reconstruction levels is finally computed as

$$N_{\mathrm{svq}} = \left(\frac{1}{L_v - 1} \cdot \frac{C_{\mathrm{svq}}}{C_g}\right)^{\frac{L_v-1}{2 \cdot L_v}} \cdot N_{\mathrm{lsvq}}^{\frac{L_v-1}{L_v}} \quad (29)$$

$$N_g = \left((L_v - 1) \cdot \frac{C_g}{C_{\mathrm{svq}}}\right)^{\frac{L_v-1}{2 \cdot L_v}} \cdot N_{\mathrm{lsvq}}^{\frac{1}{L_v}}. \quad (30)$$

As the considered quantization cell is located around the surface of the unit sphere, the variance of input signal $\mathbf{x}$ is approximately $E\{\| \mathbf{x} \|_2^2\} \approx 1$. After substituting (29) and (30) in (26), the overall logarithmic SNR in dB as a function of the overall effective bit rate $r_{\mathrm{lsvq}}$ is

$$\mathrm{SNR}_{\mathrm{lsvq}}^{(II)}\,|_{\mathrm{dB}} = 6.02 \cdot r_{\mathrm{lsvq}} - 10 \log_{10}\Bigg(\frac{L_v}{(L_v+1)^{\frac{L_v-1}{L_v}}} \cdot \left[2\sqrt{\pi}\frac{\Gamma(\frac{L_v+1}{2})}{\Gamma(\frac{L_v}{2})}\right]^{\frac{2}{L_v}} \cdot \left[\frac{(1+\ln(A))^2}{12}\right]^{\frac{1}{L_v}}\Bigg). \quad (31)$$

Considering the asymptotic case for infinite dimensions, it can be shown that

$$\lim_{L_v \to \infty} \mathrm{SNR}_{\mathrm{lsvq}}^{(II)}\,|_{\mathrm{dB}} = 6.02 \cdot r_{\mathrm{lsvq}} \quad (32)$$

which is consistent with the rate distortion function for uncorrelated Gaussian distributed sources with zero mean.

## 4. Results

The logarithmic SNR in dB for different dimensions $L_v$ and effective bit rates $r_{\mathrm{lsvq}}$ is shown in Figure 4. The curves for the "high rate approximation" are shown as solid lines with either circle, hexagram, or square markers representing the different dimensions. The dotted curves are based on the exact computation of the distortion for SVQ by numerically computing the angular radius $\gamma$ and solving the integrals in (17). For the optimal bit allocation, in both cases, instead of computing it directly according to (29) and (30), in a first step, $D_g$ is computed from $D_{\mathrm{svq}}$ according to (28). In the next step, the number of quantization reconstruction levels $N_g$ is computed from $D_g$ according to (25). Two reference curves are shown, the maximum achievable SNR for uncorrelated Gaussian distributed source with zero mean according to rate-distortion theory (RDT) which is also the asymptotic performance of LSVQ for infinite dimensions ($L_v \to \infty$) according to (32), and the performance of logarithmic (A-Law) scalar quantization as the special case of LSVQ for $L_v = 1$. The A-Law quantization constant is $A = 5000$ which is a reasonable tradeoff between dynamic range and performance of the quantizer. The fact that for infinite dimensions

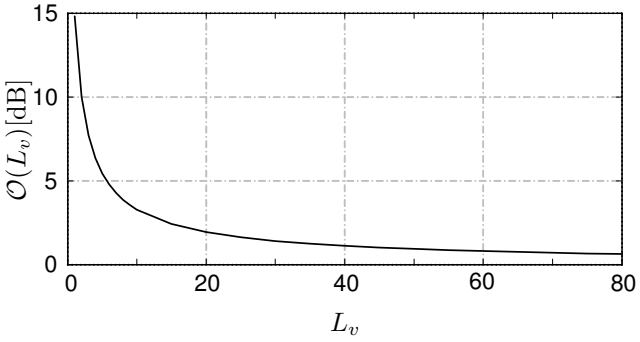


Figure 5: Logarithmic LSVQ performance offset $\mathcal{O}(L_v)$ (33) over vector dimension.

the maximum SNR according to RDT is reached is well consistent with the sphere-hardening effect mentioned in [11]. Obviously, the SNR computed according to the exact solution for SVQ (as expected) is different for low bit rates and asymptotically reaches the same performance as computed according to the high rate approximations for high bit rates. Since it is lower than the SNR related to the high rate approximation, it seems that also (23) defines a bound.
Another interesting result is shown in Figure 5 where the asymptotic SNR for infinite dimensions (32) in comparison to $\mathrm{SNR}_{\mathrm{lsvq}}^{(II)}$ for finite dimensions (31)

$$\mathcal{O}(L_v) = \lim_{L_v \to \infty} \mathrm{SNR}_{\mathrm{lsvq}}^{(II)}|_{\mathrm{dB}} - \mathrm{SNR}_{\mathrm{lsvq}}^{(II)}|_{\mathrm{dB}} \qquad (33)$$

is shown as a function of the vector dimension. For quantization in practice, this result indicates that by increasing the dimension $L_v$, the highest performance gain can be achieved in the area of low values.

## 5. Conclusion

In this paper, theoretical results for LSVQ gain-shape VQ have been presented. In the first part, a proof was given to show that LSVQ achieves a quantization SNR which is approximately independent of the input source PDF. In the second part, a lower bound for the achievable quantization SNR related to SVQ and a quantitative expression for the SNR related to LSVQ for high bit rates were derived based on assumptions similar to those known from the sphere bound for VQ in general. One important outcome of these derivations is the optimal allocation of bit rate for the logarithmic SQ of the gain and the SVQ for the shape component for high bit rates. Given a spherical code as the basis for a new LSVQ in practice, the results are a valuable reference to assess the quality of a spherical code for quantization and to find the optimal allocation of bits to gain and shape component.

## References


[1] R. Gray and D. Neuhoff, "Quantization," *IEEE Trans. Inform. Theory*, vol. 44, no. 6, pp. 2325–2383, 1998.

[2] N. Jayant and P. Noll, *Digital Coding of Waveforms*. Prentice-Hall, Inc., 1984.

[3] T. Lookabough and R. Gray, "High Resolution Quantization Theory and the Vector Quantization Advantage," *IEEE Trans. Inform. Theory*, vol. 35, no. 5, pp. 1020–1033, 1989.

[4] M. Sabin and R. Gray, "Product Code Vector Quantizers for Waveform and Voice Coding," *IEEE Trans. Acoust., Speech, Signal Processing*, vol. ASSP-32, no. 3, pp. 474–488, Jun. 1984.

[5] J. Conway and N. Sloane, *Sphere Packings, Lattices and Groups*. Springer, 1993.

[6] D. Slepian, "Permutation Modulation," *Proceedings of the IEEE*, vol. 53, no. 3, pp. 228–236, 1965.

[7] T. Berger, *Rate Distortion Theory*. Prentice-Hall, Inc., 1971.

[8] J. P. Adoul, C. Lamblin, and A. L. Guyader, "Baseband Speech Coding at 2400 bps using Spherical Vector Quantization," in *Proc. of ICASSP*, 1984.

[9] H. Krüger and P.Vary, "SCELP: Low Delay Audio Coding with Noise Shaping based on Spherical Vector Quantization," in *Proc. of EUSIPCO*, Italy, 2006.

[10] J. Hamkins, "Design and Analysis of Spherical Codes," Ph.D. dissertation, Univ. of Illinois, 1996.

[11] J. Hamkins and K. Zeger, "Gaussian Source Coding with Spherical Codes," *IEEE Trans. Inform. Theory*, vol. 48, no. 11, pp. 2980–2989, 2003.

[12] A. Gersho, "Asymptotically Optimal Block Quantization," *IEEE Trans. Inform. Theory*, vol. IT-25, no. 4, pp. 373–380, 1979.

[13] H. S. M. Coxeter, *Regular Polytopes, 3rd ed.* New York: Dover, 1973.

[14] I. N. Bronstein and K. A. Semendjajew, *Taschenbuch der Mathematik*. Teubner Verlag, 1991.